

# Molecular Alignment on Polyimide Film for Liquid Crystals by the Application of Photolithography

Halide Melik<sup>1</sup>, Mehriban Emek<sup>2</sup> and Süleyman Yılmaz<sup>1,\*</sup>

<sup>1</sup>*Harran University, Department of Physics, Osmanbey Campus, 63400 Şanlıurfa, Turkey*

<sup>2</sup>*Adıyaman University, Gölbaşı Vocational High School, 02500 Gölbaşı, Adıyaman, Turkey*

\* *Corresponding author: syilmaz@harran.edu.tr*

---

**Özet.** Bu çalışmada, polyimide ince film üzerinde moleküler yönlendirme için fotolitografi tekniği çalışıldı. Fotolitografik uygulamanın sıvı kristal yönelim özellikleri polyimide ince filmlerle sunuldu ve yüzey profilleriyle foto-yönelmiş ince polyimide film üzerinde gözlemlendi. Mikro kanal oluşturmayla sağlanan bu metot, spin kaplama, UV pozlama ve kimyasal aşındırmayı içerir. Sıvı kristal görüntüleyicinin hücre kalınlığı dönel tarama interferometrik üniteyle ölçüldü. Fotolitografik metodun sonuçları ve nematik sıvı kristal hücrenin moleküler yönelim özellikleri 100 mikronluk aralıkla oluşan mikro desenler yoluyla elektrik alan uygulanmasıyla gözlemlendi. Bu metodun ileriki çalışmalarda nano ölçekte geliştirilmesi umulmaktadır.

**Anahtar Kelimeler.** Sıvı kristaller, polyimide ince filmler, fotolitografi, moleküler yönelim.

**Abstract.** In this study, the photolithographic technique for molecular alignment on the polyimide thin film was studied. The liquid crystal alignment properties of the photolithographic application were presented by the polyimide thin films and observed on photoaligned polyimide film by a surface profiler. This method was provided by the micro-patterning process that includes spin-coating, UV exposing and wet chemical etching. The cell gap of liquid crystal displays was measured by the rotational scanning interferometer unit. The results of the photolithographic method and the molecular alignment properties of the nematic liquid crystal cell were observed by applying an electric field with the micro-patterning interval of approximately 100 microns. These results will be developed gradually in further studies for nano-scale applications.

**Keywords.** Liquid crystals, polyimide thin films, photolithography, molecular alignment.

---

## 1. Introduction

The nature of liquid crystals (LC) is very complex and their aligned surface is included in important processes such as van der Waals interactions, dipolar interactions, steric interactions, hydrogen and chemical bonding, and surface topography.

Received September 22, 2010; accepted April 25, 2011.

Basically, the molecular alignment of LCs is linked to their molecular interactions and other dynamic factors, as well as molecular anisotropy, electro-optical effects, anchoring energy, etc. The molecular alignment of LCs on treated substrates plays a very important role in basic studies and in technological applications such as mobile phones, smart cards, and integrated displays [1-4]. Alignment thin layers are extensively used in the production of liquid crystal displays (LCDs) in which the liquid crystal molecule is oriented to give a desired optical effect.

There are several molecular alignment techniques that depend on contact and non-contact procedures. The classical rubbing technique in LCDs is widely used and the best electro-optic performance is provided by this method. However, the associated impurities, electrostatic charges and mechanical damage may result in the deterioration of the quality of LC switching, particularly when active matrix elements are used for the purpose [5].

There are several types of non-contact routes for patterning alignment layers in LCDs. The patterning alignment of cinnamates and coumarins materials and special polyimide coated surfaces have been extensively investigated using micro-grooving techniques in combination with polarized light. Direct writing with low energy ion-beams on amorphous, inorganic thin films has also been used as a suitable non-contact method for pattern alignment. In particular, the micro-grooving ( $\mu$ -rubbing) method has been performed for alignment layers with an extremely sharp stylus in order to create nematic liquid crystal (NLC) devices [6-8].

At the same time, the alignment properties of photosensitive materials, such as azo-dye have been investigated recently. This alignment can be achieved using polarized UV light with high anchoring energy. Photo-alignment by photosensitive materials eliminates the generation of dust and electrostatic charges due to its non-contact nature. However, photo-alignment techniques have not yet reached an adequate quality level due to issues like the response time and contrast ratio [9].

A different technique is the photo-induced alignment technique that has been proposed to provide a homogeneous and oblique LC alignment. Photo-induced alignment includes several processes such as reversible cis-trans isomerization, photodimerization or cross-linking and photo-degradation [6]. Photo-induced alignment of LC molecules has lately attracted much attention because of its advantages over the rubbing of polyimide thin films. In this study we used the photolithography method which is provided by a micro-patterning process that includes spin-coating, UV exposure and wet chemical etching. This technique was used for the molecular alignment

because of its advantages in providing one or two division micro-scale featured patterns. In addition, this technique is also suitable because it is much simpler and cheaper than other common applications and it provided successful results.

## 2. Phase Retardation, Cell Gap and Alignment Angle

Three parameters for all LC displays are very important and significantly affect the optical properties of the LC. These are expressed as the phase retardation, the cell gap and the alignment angle of the LC molecules on the substrates. In order to optimize display performance, it is important to have an accurate and simple technique to measure the cell gap and the pretilt angle of the NLC layers.

The measurement of the LC thickness (cell gap) is an important process to determine the cell characteristics. There are various techniques to measure the gap of an empty cell, among which are the spectrum scanning method, the input polarization angle dependence method, the cross polarizer technique, and the phase compensation method [10-13]. These methods in particular depend on the categories of the single wavelength and spectral methods. The main drawback of the single wavelength method is the instability of laser power. Moreover, environmental disturbance may cause significant errors in the measurement.

In the spectrum scanning method, the measured reflectance spectrum is used to fit the twist angle  $\phi$  and retardation phase  $\Delta n \cdot d$  (where,  $\Delta n$  is the LC birefringence and  $d$  is the cell gap). The retardation value, which is very closely related to the LC transmission, can be determined by the curve fitting the theoretical curve derived from both the relational expression and the measured curve for the LC reflectance obtained with this system. The Fabry-Perot effect, owing to the inner surface reflections of ITO (indiumtin oxide), interferes with the accurate extraction of the LC phase retardation value when using the transfer calculation process of light intensity value, and hence disturbs the measurement accuracy. The crossed polarizer configuration would eliminate such an undesirable effect [12]. Generally, methods involving optics is preferred due to its simplicity and higher accuracy in comparison with the previously mentioned techniques [14].

In the measurement system of the phase retardation, the voltage-dependent phase change had to be obtained first experimentally. The maximum phase difference can be shown as follows

$$\psi_{\max} = \frac{4\pi}{\lambda}(n_e^{\text{eff}} - n_o)d \quad (1)$$

where  $n_e^{eff} = \frac{n_e n_o}{\sqrt{n_e^2 \sin^2 \theta_p + n_o^2 \cos^2 \theta_p}}$ ,  $n_e$  and  $n_o$  are the extraordinary and ordinary refractive indices of the LC material, respectively.

From the voltage dependent change of the phase retardation, the largest phase retardation was obtained and the cell gap  $d$  was then calculated with the equation

$$d = \frac{\lambda \psi_{\max}}{4\pi(n_e^{eff} - n_o)}. \quad (2)$$

In the reflected twisted nematic cell (RTNC) method, the normalized reflectance ( $R_{\perp}$ ) was obtained for the configuration of the crossed-polarizer by the Jones matrix calculus as follows

$$R_{\perp} = \left( \Gamma \frac{\sin X}{X} \right)^2 \left( \sin 2\beta \cos X - \frac{\phi}{X} \cos 2\beta \sin X \right)^2 \quad (3)$$

where  $\Gamma = 2\pi \Delta n d / \lambda$ ,  $X = \sqrt{\phi^2 + (T/2)^2}$ ,  $\beta$  is the angle between input polarizer and entrance LC director, and  $\phi$  is the twist angle of the LC. For the LC cell, the right-handed twist angle is positive and left-handed twist angle is negative.

The measurement method by LCR can be used for indirect measurement of the cell gap. The cell gap may not be uniform and the variation in gap beyond a certain percentage may show up as a change in colour, if the cell is optimized for the first minimum corresponding to the product  $(\Delta n \cdot d)$  or change in contrast. The response time is also highly affected by the cell gap ( $d$ ) and it is advisable to reject the cell if the variation in the cell gap is beyond a certain limit. The effective dielectric constants ( $\varepsilon_{eff}$ ) of the cells were computed using the following equation

$$\varepsilon_{eff} = \frac{Cd}{\varepsilon_0 S_{electrode}} \quad (4)$$

where  $C$  is the capacitance of the cell,  $d$  is the cell gap and  $S$  is the area of cross-section of the electrodes.

As an alternative, interferometric measuring is a very suitable method that is based on the transmission curve by the rotational interferometer. The light travels through an empty cell, and the transmitted light is changed with the angular rotation. The angles are determined by the angular distribution of the transmitted light due to the maximum points. Thus, these obtained values are used according to the following formula to calculate the thickness of the empty cell

$$d = \frac{\Delta m \lambda}{2(\cos \theta_2 - \cos \theta_1)} \quad (5)$$

where  $\Delta m$  is the number of minima between the two chosen peaks and in the transmittance curve two peaks with angles  $\theta_1$  and  $\theta_2$ , respectively.

Another important result of the molecular alignment is determining the pretilt angle of the molecular orientation. The crystal rotation method was used in industrial applications. The cell is placed between two polarizers. A monochromatic light source is used, a rotating stage turns the cell and a photo-diode measures the interference intensity. ELDIM uses another method to determine the tilt bias angle of an anti-parallel LC cell using our EZContrast System. The cell to be tested is located between two crossed or parallel polarizers, oriented at  $45^\circ$  from the principal plane of the cell. This plane is defined by the surface as normal and the optical axis of the LC. The sample is illuminated by the diffused light source and the cell is located before EZContrast objective. The principle of the measurement consists in analyzing the interference figure at an infinite distance, i.e. in the Fourier plane of the EZContrast, for a given wavelength. The orientation of the director [15], which is the average direction of the long axis of the LC molecules, can be obtained as follows

$$\theta = \sin^{-1} \sqrt{\frac{\varepsilon_{eff} - \varepsilon_{\perp}}{\varepsilon_{\parallel} - \varepsilon_{\perp}}} \quad (6)$$

where  $\varepsilon_{\parallel}$  and  $\varepsilon_{\perp}$  are dielectric constant due to the parallel and perpendicular polarization states, respectively.

To illustrate the measuring of the pretilt angle, the NLC directors were assumed to be uniformly parallel aligned in the absence of an electric field. To simplify the mathematical analysis, a new variable  $\phi$  was defined as  $\sin \theta = \sin \theta_{\max} \sin \phi$ . Using this new variable, we obtained

$$d\theta = \frac{\sqrt{\sin^2 \theta_{\max} - \sin^2 \theta}}{\sqrt{1 - \eta \sin^2 \phi}} d\phi \quad (7)$$

where  $\eta = \sin^2 \theta_{\max}$ .

Together with the pretilt angle, the anchoring energy  $W$  is one of the most important properties describing the alignment of the LC. The anchoring energy is described by the interactions strength between LC and the alignment material or how easy it is to change the alignment of the LC director at the surface to a preferred direction. The anchoring energy is formed from two parts due to the interaction between surface and molecules; one is the polar anchoring energy,  $W_{\theta}$ , and the other is azimuthal anchoring energy,  $W_{\phi}$  [16]. The properties of the LCD strongly depend on the

interaction between LC molecules and the surface. Finally, it is defined as

$$W(\theta, \phi) = \frac{1}{2}W_\theta \sin^2 \theta + \frac{1}{2}W_\phi \sin^2 \phi \quad (8)$$

where  $\theta$  and  $\phi$  are the polar and the azimuthal angles from the preferred direction at the surface, respectively.

To investigate the relation between the order parameter and the alignment properties of NLCs on the film, various LCDs were fabricated. The surface anchoring for a none-polar LC is generally characterized by two parts: one of the is the component of azimuthal anchoring, which governs the anchoring with respect to the plane twist of the NLC and the other is a polar anchoring term, which controls the out of plane tilt. The torque balance equation helps to estimate the azimuthal anchoring strength  $W_\phi$ , as the actual twist angle should be less than that prepared in the experiment [17]

$$W_\phi = \frac{2K_{22}\phi}{d \sin(\phi_0 - \phi)} \quad (9)$$

where  $\phi_0$ ,  $K_{22}$ , and  $d$  are the twist angle prepared in the experiment, the actually measured twist angle, the twist elastic constant of a liquid crystal, and the cell gap, respectively. To measure the polar anchoring energy  $W_\theta$  of the alignment film and LC interface, the simplified high electric field technique (HEFT) was used [18]. Thus, the polar anchoring energy is calculated from the extrapolation length according to

$$W_\theta = \frac{K_{11} \sin^2 \theta_e + K_{33} \cos^2 \theta_e}{d_e} \quad (10)$$

where  $K_{11}$  and  $K_{33}$  are the splay and bend elastic constant of the LC material, respectively, and  $\theta_e$  is the pretilt angle.

It was found that the behaviour of the polar anchoring energy with respect to the UV exposure dose is similar to that of the azimuthal anchoring energy at the saturation level. At the boundary, the director deviates from the direction of the grooves by an angle  $\delta$  due to the spontaneous twisting power of the chiral-doped nematic LC. The anchoring strength  $A$  is defined by the free surface energy  $F_s$  using the following equation

$$F_s = \frac{1}{2}A \sin^2 \delta \quad (11)$$

where  $A$  is the anchoring strength. By the total twist angle  $\theta$  in the cell, the transmission  $T$  can be written as follows [19,20]

$$T = \left[ \frac{1}{\sqrt{1+u^2}} \sin(\sqrt{1+u^2}\theta) \sin(\theta - \psi_{pol}) + \cos(\sqrt{1+u^2}\theta) \cos(\theta - \psi_{pol}) \right]^2 + \frac{u^2}{1+u^2} \sin^2(\sqrt{1+u^2}\theta) \cos^2(\theta + 2\psi_0 - \psi_{pol}) \quad (12)$$

and

$$u = \frac{\pi d}{\lambda \theta} (n_e - n_o) \quad (13)$$

where  $\psi_0$  and  $\psi_{pol}$  are the angles of the LC director at the first surface and the analyzer, respectively, with respect to the polarizer,  $n_e$  and  $n_o$  are the extraordinary and ordinary refractive indices of the LC and  $\lambda$  is the wavelength of incident light ( $\lambda=632.8$  nm for He-Ne). The value of transmittance reaches its absolute minimum with respect to the two variables,  $\psi_0$  and  $\psi_{pol}$ , where both of the two terms in (12) are zero, i.e., the two following conditions

$$\frac{1}{\sqrt{1+u^2}} \sin(\sqrt{1+u^2}\theta) \sin(\theta - \psi_{pol}) + \cos(\sqrt{1+u^2}\theta) \cos(\theta - \psi_{pol}) = 0 \quad (14)$$

and

$$\theta + 2\psi_0 - \psi_{pol} = \pm \frac{\pi}{2} \quad (15)$$

are satisfied. With the deduced twist angle  $\theta$ , the azimuthal anchoring strength,  $A$  was then obtained as follows

$$A = \frac{2K_{22}}{\sin \theta} \left( \frac{2\pi}{P_0} - \frac{\theta}{d} \right) \quad (16)$$

where  $K_{22}$  is the twist elastic constant.

When the substrate is illuminated at normal incidence, no pretilt angle is defined. In order to generate a pretilt angle, oblique exposure is needed. For this purpose, two different methods are suitable. In the first one, the substrate is illuminated with oblique spherically polarized light at  $45^\circ$  angle of incidence. In the second, a two-step exposure is performed. Thus, the substrate is exposed to polarized UV light at normal incidence, aligning the randomly oriented molecules and then an obliquely unpolarized exposure is applied, causing the pretilt angle generation.

### 3. Photolithographic Applications and Experimental Results

It is well known that the polyimide is a suitable material for coating on the surface as alignment material which has the high cure temperatures ( $\sim 350^\circ\text{C}$ ). Polyimide exhibits imidisation properties much faster than other standard products at lower temperatures. Especially, it has supplied viscous solutions very suitable for spin or roller coating applications. Processing by wet or plasma etch is possible with these materials and a cured film thickness from  $0.5\ \mu\text{m}$  to  $6\ \mu\text{m}$  can be obtained. Because of their excellent properties such as high refractive index, adhesion to the substrates, high resistivity, excellent transparency in the visible spectrum, and high chemical and thermal stability, they are usually preferred as the aligned surfaces.

Spin coating by the adhesion promoter precursor was performed with spin dry 5000 rpm on the ITO glass substrates by using a Spin-Coater. The polyimide coating was performed in two steps by rotating at 500 rpm and at final speed rpm. The photo-resist material was coated on the surface of the polyimide film by spinning at 500 rpm and at final speed rpm with spin-drying. The coated layer was exposed to UV light (Figure 1) with a wavelength of 320 nm and power of  $9.850\ \text{mWcm}^{-2}$ .

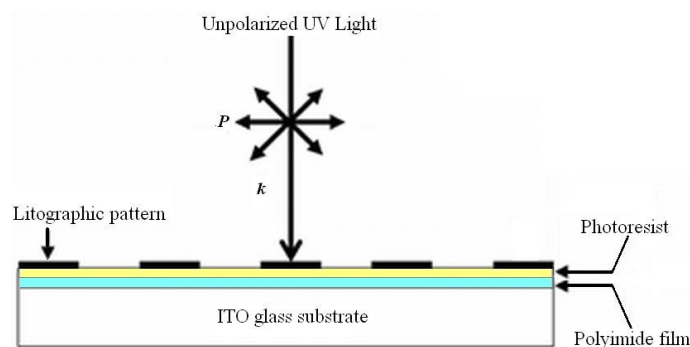


FIGURE 1. Schematic representation of photo-chemical reactions for photo-induced alignment.

After UV exposure, the alignment surface is ready for the development procedure. The development process is very important in order to remove contaminated materials from the surface and this is the so-called wet chemical etching process. The last application of the coated substrate was completed by curing with a suitable heating and cooling system. The two antiparallel substrates were assembled using fast drying epoxy adhesive material and spacer (fibre wires with  $30\ \mu\text{m}$ ). This study was extended in order to measure the electro-optic performance of homogeneously

aligned samples. Antiparallel substrates were made with the above-mentioned lithographic patterning with a cell thickness of  $\sim 40 \mu\text{m}$ . The cell was placed perpendicular between cross polarizers for the electro-optical measurements (Figure 2). The alternating exposed and unexposed lithographic patterns can be clearly seen by polarized microphotographs of a photo-aligned LC cell between crossed polarizers. The exposed region produces a random planar alignment with NLC texture of 8CB (Figure 3).

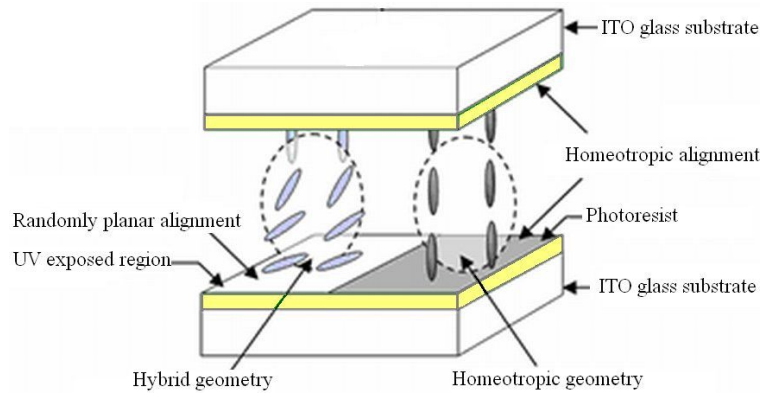


FIGURE 2. The photo-aligned liquid crystal cell with an alternating exposed and unexposed region by lithographic pattern.

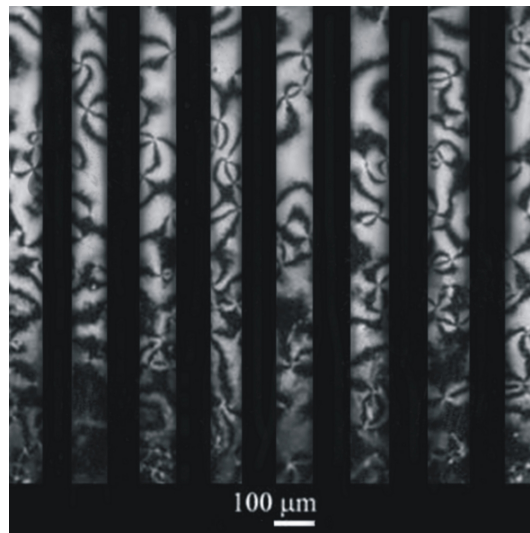


FIGURE 3. Microphotographs of a photo-aligned nematic liquid crystal (8CB) cell by planar alignment.

## 4. Conclusions

In this study, the photolithographic technique was used for molecular alignment, which is very attractive application for improving on the conventional molecular alignment. We noted that this technique provides a controllable pretilt angle and strong anchoring energy of the LC cell, as well as having high thermal and ultraviolet (UV) stability. Its unique features and alignment properties provided potentially good results with large scale advantages and promises high production through the placing of alignment layers in LCDs. It was inferred that the photolithographic method also offers a better control of the homeotropic alignment, as well as planar alignment. An ideally aligned surface was provided by the suitable lithographic pattern and enough exposure time, photo-resist thickness, etching time, developer percentage, etc. Future developments of the photolithographic technique for the nano-scale can be expected to produce promising applications using nano-patterning applications.

**Acknowledgment.** The authors thank TUBITAK for funding and thank Professor Christ Glorieux, Dr. Jan Leys and Dr. Kanhaiya Ojha from the Catholic University of Leuven, Belgium, for collaboration during this study. The authors also thank Dr. Muharram Zarbaliyev and Dr. Nurettin Besli from Harran University, Turkey, for their review.

## References

- [1] P. Slikkerveer, P. Bouten, P. Cirkel, J. de Goede, H. Jagt, N. Kooyman, G. Nisato, R. van Rijswijk and P. Duineveld, 16.2: A fully flexible colour display, *SID Symposium Digest of Technical Papers* **35** (2004), 770–773.
- [2] S. Varghese, S. Narayanankutty, C. W. M. Bastiaansen, G. P. Crawford and D. J. Broer, Patterned alignment of liquid crystals by  $\mu$ -rubbing, *Advanced Materials* **16** (2004), 1600–1605.
- [3] J. Osterman, C. Adås, L. Madsen and K. Skarp, P-124: Properties of azo-dye alignment layer on plastic substrates, *SID Symposium Digest of Technical Papers* **36** (2005), 772–775.
- [4] V. Konovalov, V. Chigrinov, H. S. Kwok, H. Takada and H. Takatsu, Photoaligned vertical aligned nematic mode in liquid crystals, *Japanese Journal of Applied Physics* **43** (2004), 261–266.
- [5] V. G. Chigrinov, *Liquid Crystal Devices: Physics and Applications*, Artech House, Boston 1999.
- [6] M. O’Neill and S. M. Kelly, Photoinduced surface alignment for liquid crystal displays, *Journal of Physics D: Applied Physics* **33** (2000), R67.

- [7] M. Schadt, H. Seiberle and A. Schuster, Optical patterning of multi-domain liquid-crystal displays with wide viewing angles, *Nature* **381** (1996), 212–215.
- [8] R. Yamaguchi, Y. Goto and S. Sato, A novel patterning method of liquid crystal alignment by azimuthal anchoring control, *Japanese Journal of Applied Physics* **41** (2002), L889–L891.
- [9] R. Karapinar, M. O'Neill, S. M. Kelly, A. W. Hall and G. J. Owen, Molecular alignment of liquid crystals on a photosensitive polymer surface exposed to linearly polarised ultraviolet laser radiation, *ARI - An International Journal for Physical and Engineering Sciences* **51** (1998), 61–65.
- [10] G.-D. Lee, T.-H. Yoon and J. C. Kim, Cell gap measurement method for single-polarizer reflective liquid crystal cells, *Japanese Journal of Applied Physics* **40** (2001), 3330–3331.
- [11] S.-T. Wu and G. Xu, Cell gap and twist angle determinations of a reflective liquid crystal display, *IEEE Transactions on Electron Devices* **47** (2000), 2290–2293.
- [12] X. Zhu, W.-K. Choi and S.-T. Wu, A simple method for measuring the cell gap of a reflective twisted nematic LCD, *IEEE Transactions on Electron Devices* **49** (2002), 1863–1867.
- [13] H. L. Ong, 26.1: Simple and accurate optical reflection and phase compensation methods for reflective LCD cell gap, *SID Symposium Digest of Technical Papers* **32** (2001), 430–433.
- [14] S. J. Hwang, S.-T. Lin, C.-H. Lai, A novel method to measure the cell gap and pretilt angle of a reflective liquid crystal display, *Optics Communications* **260** (2006), 614–620.
- [15] H. J. Deuling, Deformation of nematic liquid crystals in an electric field, *Molecular Crystals and Liquid Crystals* **19** (1972), 123–131.
- [16] J. Osterman, *Investigations of Optical Properties and Photo-Alignment in Bistable Nematic Liquid Crystal Displays*, PhD. Thesis, Upsala University, Uppsala 2005.
- [17] V. Vorflusev, H.-S. Kitzerow and V. Chigrinov, Azimuthal anchoring energy in photoinduced anisotropic films, *Japanese Journal of Applied Physics* **34** (1995), L1137–L1140.
- [18] H. Yokoyama and R. Sun, Simplified high-electric-field technique for measuring the liquid crystal anchoring strength, *Japanese Journal of Applied Physics* **39** (2000), L45–L47.
- [19] Y.-F. Lin, M.-C. Tsou and R.-P. Pan, Alignment of liquid crystals by ion etched grooved glass surfaces, *Chinese Journal of Physics* **43** (2005), 1066–1073.
- [20] H. Hah, S.-J. Sung, M. Han, S. Lee and J.-K. Park, Effect of the shape of imprinted alignment layer on the molecular orientation of liquid crystal, *Materials Science and Engineering: C* **27** (2007), 798–801.

